EUROPEAN JOURNAL OF PURE AND APPLIED MATHEMATICS
2025, Vol. 18, Issue 2, Article Number 6186
ISSN 1307-5543 – ejpam.com
Published by New York Business Global

A Computational Analysis of Convection-Diffusion Model with Memory Using the Caputo-Fabrizio Derivative and Cubic Trigonometric B-Spline Functions

Mehwish Saleem[1], Arshed Ali[1], Imtiaz Ahmad[2,3,*], Aziz Khan[4], Thabet Abdeljawad[4,*]

[1] *Department of Mathematics, Islamia College Peshawar, Khyber Pakhtunkhwa, Pakistan*
[2] *Department of Mathematics, Saveetha School of Engineering (SIMATS), Thandalam 600124, Chennai, Tamil Nadu, India*
[3] *Institute of Informatics and Computing in Energy (IICE), Universiti Tenaga Nasional (UNITEN), Kajang 43000, Selangor, Malaysia*
[4] *Department of Mathematics and Sciences, Prince Sultan University, P.O. Box 66833, 11586 Riyadh, Saudi Arabia*

Abstract. This paper presents the first study on computational solutions for time-fractional partial integro-differential equations (PIDE) arising from convection-diffusion processes with memory, employing the Caputo-Fabrizio fractional derivative and the cubic trigonometric B-spline differential quadrature method. The first order backward finite difference formula is used to evaluate the Caputo-Fabrizio derivative, converting the PIDE into an integro-differential equation (IDE). The cubic trigonometric B-spline-based differential quadrature method is applied to approximate the spatial derivatives, transforming the IDE into a system of algebraic equations by expressing spatial derivatives as a weighted sum of function values. The weighting coefficients are obtained using an efficient tridiagonal solver. The method is validated through three test problems, and its computational efficiency, stability,and numerical convergence are analyzed. The results are also compared with those obtained using the cubic B-spline collocation method.

2020 Mathematics Subject Classifications: 35R11, 65M70,45J05, 65M06, 35K05

Key Words and Phrases: Caputo-Fabrizio fractional derivative, Cubic trigonometric B-spline functions, Fractional partial integro-differential equation, Convection-Diffusion process

1. Introduction

Fractional calculus has gained significant attention from researchers over the last two decades because of its ability to model non-classical phenomena accurately and reliably across various scientific fields. These include applications in areas such as viscoelastic

*Corresponding author.
*Corresponding author.
DOI: https://doi.org/10.29020/nybg.ejpam.v18i2.6186

Email addresses: imtiazkakakhil@gmail.com (I. Ahmad), tabdeljawad@psu.edu.sa (T. Abdeljawad)

materials in polymers, motion of an immersed plate, gas flow in fluids, heat flux intensity in blast furnace walls, radiation cooling of a semi-infinite body, acoustic dissipation, rheology, neutron transport in nuclear reactors, self-focusing in laser pulses, materials with thermal resistance, electrical circuits with fractance, dynamical system controllers, and the mechanical and electrical properties of real materials [1–5]. Similarly to classical (integer-order) calculus, fractional (noninteger-order) calculus also has a long-standing history. In fact, fractional calculus generalizes classical calculus. The key advantage of fractional differential operators is that, unlike integer-order differential operators, they do not overlook the effects of memory and inherited properties within the underlying model, thereby providing a more accurate definition of the process. Additionally, classical derivatives are local in nature, failing to capture processes and systems with dynamic memory and spatial nonlocality. In contrast, fractional derivatives inherently possess the feature of nonlocality [6–10].

The Caputo fractional derivative, introduced by Caputo in 1960 [11], is one of the most widely used fractional differentiation operators that depends on the singular kernel.The advantage of this definition is that it facilitates the inclusion of easily interpretable initial conditions in addition that the derivative of a constant is zero. However, the singular kernel in Caputo definition is a vital complexity and cognitive complication in the solution of fraction order differential equations [12–16]. In 2015, Caputo and Fabrizio [17] proposed a novel fractional derivative with a non-singular kernel to circumvent this difficulty. In addition to this property, the Caputo-Fabrizio derivative possesses several notable characteristics, including its ability to model material heterogeneities configurations with different scales which are similar to Caputo derivative. There has been observed considerable progress in realization of the Caputo-Fabrizio fractional derivative, leading to several significant advancements in its theory and applications in real wold problems. Losada and Nieto [18] founded the Caputo-Fabrizio integral, and application of this integral in the solution of linear and nonlinear fractional differential equations involving Caputo-Fabrizio and fractional falling body problem. Atangana and Alkahtani [19] successfully translated a resistance, inductance, capacitance circuit from ordinary equation to fractional differential equation by using Caputo-Fabrizio derivative in order to include the parameter to describe the low or high flow of electricity. Gómez-Aguilar et al. [20] modeled and analyzed the mass-spring-damper systems with different source terms to examine the displacement of the oscillator in fractal geometries, by using the Caputo-Fabrizio approach. Atangana and Alqahtani [21] developed numerical methods for time fractional and space fractional Caputo-Fabrizio derivatives and implemented by solving fractional advection diffusion model. Abdeljawad and Baleanu [22] provided the integration by parts formula and discrete version for Caputo-Fabrizio derivative using discrete exponential kernel. Al-Refai [23] derived a closed form reduction order formula for Caputo-Fabrizio derivative to get second linearly independent solution of linear fractional differential equations. Ypez-Martnez and Gómez-Aguilar [24] presented a modified definition of Caputo-Fabrizio fractional-order operator and some properties of this definition to solve non-linear polynomial type fractional differential equations using analytical methods. Qureshi et al. [25] obtained a first-order formula for Capto-Fabrizio derivative and applied to diffusion-wave equation. Jassim and

Hussain [26] compared the approximate analytical solutions of the fractional system of differential equations with Caputo-Fabrizio fractional derivative operator obtained using two approximate analytical methods. Jin et al. [27] examined the dynamic behavior of the drinking population through the Caputo-Fabrizio fractional drinking model. Jamil et al. [28] analyzed Caputo-Fabrizio based non-Newtonian magnetic Casson blood flow in an inclined stenosed artery. Adel et al. [29] discussed full-number solicitation model for the spread of corona virus in COVID-19 pandemic. Ahmad et al. [30] investigate the dynamical behavior of the Hepatitis B virus using the Caputo-Fabrizio fractional derivative. Dehingia et al. [31] investigate the dynamics of a nutrient-plankton system by incorporating Caputo and Caputo-Fabrizio fractional operators. Chauhan et al [32] provided Caputo-Fabriio based system for the dynamics and behavior of a financial model. Kausar et al. [33] introduced a nonlinear fractional circuits modeling using a stochastic neuro-computational artificial intelligent-based Caputo-Fabrizio stiff electric circuit model. Güngör [34] studied the Caputo-Fabrizio fractional Cahn-Allen equation using the Caputo-Fabrizio q-Elzaki homotopy analysis transform method.

Physical phenomena that involve memory and inherited characteristics are frequently modeled in physics and engineering through partial integro-differential equations (PIDEs) (see [35–37] and references therein). With the growing interest in fractional derivatives, numerous linear and nonlinear PIDEs have been investigated using these derivatives. These include PIDE models that describe heat transfer in materials with memory [38], viscoelasticity [39], transonic multiphase flows [40] and thin beam and plate structures [41]. Finding exact analytical solutions for fractional PIDEs is generally difficult, thus numerical methods play a crucial role in solving these equations [36]. Hussain et al. [38] used the variational iteration method to numerically solve fractional PIDEs. Saima [42] used the cubic B-spline collocation method to solve a second-order time-fractional PIDE. Avazzadeh et al. [39] applied Legendre wavelets to solve a fractional viscoelastic PIDE. Bazgir and Ghazanfari [41] presented a solution for fourth-order fractional PIDEs with a singular kernel through a mixed spectral method. Arqub [40] solved various time-fractional PIDEs using the iterative reproducing kernel method. Loha et al. [43] provided an approximate solution for a class of time-fractional PIDEs. Guo et al. [44] solved a nonlinear time-fractional PIDE using the iterative finite difference method. Tayabba et al. [45] developed an extended cubic B-spline collocation method along with Newton's linearization technique for nonlinear time-fractional PIDEs. Atta and Youssri [46] proposed the spectral Chebyshev collocation method to solve a time-fractional nonlinear PIDE with a weakly singular kernel. Luo et al. [47] introduced a new compact difference scheme based on the shifted and weighted Grünwald formula for time-fractional PIDEs. Mohapatra et al. [48] found the solution of time-fractional PIDE using the Adomian decomposition method and the homotopy perturbation method. Recently, Panda and Mohapatra implemented three semi-analytical techniques to solve a time-fractional PIDE. In this paper, the following PIDE with the Caputo-Fabrizio fractional derivative is considered:

$$ {}_0^{CF}D_t^{\alpha}v(\xi,t)+\lambda\frac{\partial v(\xi,t)}{\partial \xi}-\eta\frac{\partial^2 v(\xi,t)}{\partial \xi^2} = \int_0^{\mathtt{t}} (\mathtt{t}-p)^{-\beta}v(\xi,p)dp+q(\xi,\mathtt{t}), \xi\in\Omega, \mathtt{t}>0,\ 0<\alpha<1, \tag{1} $$

subject to initial condition

$$ v(\xi,0)=\delta_1(\xi),\ \xi\in\Omega,\ t>0, \tag{2} $$

and boundary conditions

$$ v(\gamma_1,t)=\lambda_1(t), v(\gamma_2,t)=\lambda_2(t),\ t>0, \tag{3} $$

where $\Omega=[\gamma_1,\gamma_2]$, $q(\xi,\mathtt{t})$ is a known function, and $\int_0^{\mathtt{t}}(\mathtt{t}-p)^{-\beta}v(\xi,p)dp$ is the memory term, λ_1,λ_2 are boundary operators, ${}_0^{CF}D_t^{\alpha}$ is the Caputo-Fabrizio fractional derivative, λ,η are convection and diffusion coefficients respectively. For the integer-order case that is for $\alpha=1$, Eq.(1) is solved by different methods including cubic B-spline collocation method (CBSCM) [49], quartic B-spline collocation technique [50], radial basis collocation method [51], sinc collocation method product trapezoidal [52], cubic B-spline Galerkin method with quadratic weight function [53] and cubic trigonometric B-spline collocation method [54].

Computational methods are widely used to provide a systematic and efficient way to solve complex problems that arise in several fields, including engineering, science, social sciences, and economics. These methods utilize mathematical models, algorithms, and numerical techniques to simulate, analyze, and predict the behavior of systems that may be difficult or impossible to solve analytically. Cubic trigonometric B-spline (CTBS) functions spans a variety of fields that require smooth, flexible, and computationally efficient solutions for approximating, interpolating, or modeling data. Some important features of these functions are smoothness, nonnegativity, design and analysis of shape of curve, partition of unity, extension of solution to the entire spatial domain, C^2 continuity, and recurrence relation. Recently, different fractional differential equations have been solved using CTBS based methods, including the fractional diffusion wave equation [55], the fractional Burger equation [56], the fractional telegraph equation [57], the fractional diffusion equation [58], time-fractional Schrödinger equation [59], and the time-fractional gas dynamics problem [60].

Upto the best of our knowledge, computational solution of the time-fractional PIDEs using Caputo-Fabrizio fractional derivative is not yet studied, which is the significance of the present work.

The remaining portion of the paper is outlined as: Section 1 provides an introduction and some preliminaries on the Caputo-Fabrizio fractional derivative and CTBS functions. Section 2 presents the development of the proposed method using the Caputo-Fabrizio fractional derivative, backward difference formula, differential quadrature, and CTBS functions. Section 3 focuses on the stability analysis of the proposed schemes. Section 4 presents numerical results, including error norms, computational efficiency, spectral radii, numerical convergence, and a comparison with an existing method to evaluate the performance of the current approach. The paper's findings are summarized in Section 5.

In this work we use the following notions to obtain the proposed scheme:
Definition [17, 21, 61]: The fractional order Caputo-Fabrizio derivative ${}_0^{CF}D_t^{\alpha} f(t)$ is defined by:

$$ {}_0^{CF}D_t^{\alpha} f(t) = \frac{M(\alpha)}{1-\alpha} \int_0^t \exp\left(\frac{-\alpha}{1-\alpha}(t-p)\right) f'(p)dp,\ 0<\alpha<1, $$

where $f \in H^1(0,t)$ and $M(\alpha)$ is a normalization function such that $M(0) = M(1) = 1$.
Theorem [17, 21]: Let function $f(t)$ be a function in $C^2[0,T]$, then the Caputo-Fabrizio derivative has first-order approximation at a point $t^j = j\delta t$, with $f^j = f(t^j), j = 0,1,2,...,s$ is defined as:

$$ {}_0^{CF}D_t^{\alpha} f(t^s) = \frac{M(\alpha)}{\alpha} \sum_{j=1}^{s} \left(\frac{f^{j+1}-f^j}{\delta t}\right) d_{j,\delta t} + O(\delta t^2),\ 0<\alpha<1, \tag{4} $$

with $d_{j,\delta t} = \exp\left(-\alpha\frac{\delta t}{1-\alpha}(s-j-1)\right) - \exp\left(-\alpha\frac{\delta t}{1-\alpha}(s-j)\right)$.

2. The Proposed Method

2.1 Temporal Approximation

We approximate the problem in time, taking $t = t^{s+1}$, $s = 0,1,2,...,M$, in Eq. (1) as,

$$ \frac{\partial^{\alpha} v(\xi,\mathsf{t}^{s+1})}{\partial \mathsf{t}^{\alpha}} + \lambda\frac{\partial v(\xi,t^{s+1})}{\partial \xi} - \eta\frac{\partial^2 v(\xi,t^{s+1})}{\partial \xi^2} = \int_0^{t^{s+1}} (t^{s+1}-p)^{-\beta} v(\xi,p)dp + q(\xi,t^{s+1}). \tag{5} $$

The time fractional derivative $\frac{\partial^{\alpha} v(\xi,\mathsf{t}^{s+1})}{\partial \mathsf{t}^{\alpha}}$ in (5) is approximated using (4) as follows:

$$ \begin{aligned} \frac{\partial^{\alpha} v(\xi,\mathsf{t}^{s+1})}{\partial \mathsf{t}^{\alpha}} &= \frac{M(\alpha)}{\alpha\delta t} \sum_{j=0}^{s} \left(v(\xi,t^{s+1}) - v(\xi,t^s)\right)\left(\exp\left(-\alpha\frac{\delta t}{1-\alpha}(s-j+1)\right) - \exp\left(-\alpha\frac{\delta t}{1-\alpha}(s-j)\right)\right) \\ &= \frac{M(\alpha)}{\alpha\delta t} \sum_{j=0}^{s} \mu_j (v(\xi,t^{s-j+1}) - v(\xi,t^{s-j})), \\ &= \frac{M(\alpha)}{\alpha\delta t}\left(\mu_0 v(\xi,\mathsf{t}^{s+1}) + \sum_{j=0}^{s-1}(\mu_{j+1}-\mu_j)v(\xi,t^{s-j}) + \mu_s v(\xi,t^0)\right), \end{aligned} $$

where $\mu_j = \left(\exp\left(\frac{-\alpha}{1-\alpha}(j\delta t)\right) - \exp\left(\frac{-\alpha}{1-\alpha}((j+1)\delta t)\right)\right)$, $j = 0, 1, 2, ..., s$.
To evaluate the integral term in Eq. (5), we proceed as follows:

$$\begin{aligned}\int_0^{t^{s+1}} (t^{s+1} - p)^{-\beta} v(\xi, p) dp &= \sum_{j=0}^{s} \int_{t^j}^{t^{j+1}} p^{-\beta} v(\xi, t^{s+1} - p)\, dp \\ &= \sum_{j=0}^{s} v(\xi, t^{s-j+1}) \int_{t^j}^{t^{j+1}} p^{-\beta}\, dp \\ &= \frac{\delta \mathsf{t}^{1-\beta}}{1-\beta} \sum_{j=0}^{s} \nu_j v(\xi, t^{s-j+1}),\end{aligned}$$

where $\nu_j = \left((j+1)^{1-\beta} - j^{1-\beta}\right)$, $j = 1, 2, ..., s, \nu_0 = 1$.
Substituting these approximations in Eq. (5), we have

$$\begin{aligned}&\frac{M(\alpha)}{\alpha\delta t}\left(\mu_0 v(\xi, \mathsf{t}^{s+1}) + \sum_{j=0}^{s-1}(\mu_{j+1} - \mu_j) v(\xi, t^{s-j}) - \mu_s v(\xi, t^0)\right) + \lambda \frac{\partial v(\xi, t^{s+1})}{\partial \xi} - \eta \frac{\partial^2 v(\xi, t^{s+1})}{\partial \xi^2} \\ &= \frac{\delta \mathsf{t}^{1-\beta}}{1-\beta} \sum_{j=0}^{s} \nu_j v(\xi, t^{s-j+1}) + q(\xi, t^{s+1}).\end{aligned} \tag{6}$$

Rearranging the terms in Eq. (6),

$$\begin{aligned}&\left(1 - \frac{\alpha\delta \mathsf{t}^{2-\beta}}{\mu_0 M(\alpha)(1-\beta)}\right) v(\xi, \mathsf{t}^{s+1}) + \frac{\alpha\delta \mathsf{t}}{\mu_0 M(\alpha)}\left(\lambda \frac{\partial v(\xi, t^{s+1})}{\partial \xi} - \eta \frac{\partial^2 v(\xi, t^{s+1})}{\partial \xi^2}\right) = \left(\frac{\mu_0 - \mu_1}{\mu_0}\right) v(\xi, t^s) + \\ &\sum_{j=1}^{s-1}\left(\frac{\mu_j - \mu_{j+1}}{\mu_0}\right) v(\xi, t^{s-j}) + \left(\frac{\mu_s}{\mu_0} v(\xi, t^0)\right) + \frac{\alpha\delta t^{2-\beta}}{\mu_0 M(\alpha)(1-\beta)}\left(\sum_{j=1}^{s} \nu_s v(\xi, t^{s-j+1}) + q(\xi, t^{s+1})\right).\end{aligned} \tag{7}$$

2.2 Approximation in Space

We now approximate the solution in space dimension. The differential quadrature method [36] provides kth order derivative of the function $v(\xi, \mathsf{t})$ from the values of $v(\xi, \mathsf{t})$ at $\xi_r, r \in I_1 = \{1, 2, ..., N\}$, as

$$\frac{\partial^k v(\xi_r, \mathsf{t})}{\partial \xi^k} = \sum_{r=1}^{N} a_{rs}^{(k)} v(\xi_s, \mathsf{t}), \tag{8}$$

where $a_{rs}^{(k)}$, $k = 1, 2, ...$ are kth order weighting coefficients which are determined by test

functions (for detail see [36]). Now taking $\xi = \xi_r$ and using (8) in (7), we get

$$\left(1 - \frac{\alpha\delta \mathrm{t}^{2-\beta}}{\mu_0 M(\alpha)(1-\beta)}\right) v(\xi_r, \mathrm{t}^{s+1}) + \frac{\alpha\delta \mathrm{t}}{\mu_0 M(\alpha)} \left(\lambda \sum_{m=1}^{N} a_{rm}^{(1)} v(\xi_m, t^{s+1}) - \eta \sum_{m=1}^{N} a_{rm}^{(2)} v(\xi_m, t^{s+1})\right)$$
$$= \left(\frac{\mu_0 - \mu_1}{\mu_0}\right) v(\xi_r, t^s) + \sum_{j=1}^{s-1} \left(\frac{\mu_j - \mu_{j+1}}{\mu_0}\right) v(\xi_r, t^{s-j}) + \left(\frac{\mu_s}{\mu_0} v(\xi_r, t^0)\right)$$
$$+ \frac{\alpha\delta t^{2-\beta}}{\mu_0 M(\alpha)(1-\beta)} \left(\sum_{j=1}^{s} \nu_s v(\xi_r, t^{s-j+1}) + q(\xi_r, t^{s+1})\right). \tag{9}$$

To obtain the weighting coefficients $a_{rm}^{(1)}, a_{rm}^{(2)}$, $r, m = 1, 2, ..., N$ in Eq. (2), the following modified CTBS functions are used [62]:

$$\begin{aligned} S_1(\xi) &= \mathcal{T}_1(\xi) + 2\mathcal{T}_0(\xi), \\ S_2(\xi) &= \mathcal{T}_2(\xi) - \mathcal{T}_0(\xi), \\ S_l(\xi) &= \mathcal{T}_l(\xi), \text{for } l = 3, 4, ..., N-2, \\ S_{N-1}(\xi) &= \mathcal{T}_{N-1}(\xi) - \mathcal{T}_{N+1}(\xi), \\ S_N(\xi) &= \mathcal{T}_N(\xi) + 2\mathcal{T}_{N+1}(\xi), \end{aligned}$$

which form a basis in region Ω and the CTBS functions are defined by

$$\mathcal{T}_r(\xi) = \frac{1}{\theta} \begin{cases} \sin^3(\frac{\xi - \xi_{r-2}}{2}), & \xi \in \Omega_{r-1}, \\ [\sin(\frac{\xi-\xi_{r-2}}{2}) \sin(\frac{\xi_r - \xi}{2}) + \\ \sin(\frac{\xi_{r+1}-\xi}{2}) \sin(\frac{\xi-\xi_{r-1}}{2})] \sin(\frac{\xi-\xi_{r-2}}{2}) + \sin^2(\frac{\xi-\xi_{r-1}}{2}) \sin(\frac{\xi_{r+1}-\xi}{2}), & \xi \in \Omega_r, \\ \sin(\frac{\xi-\xi_{r-2}}{2}) \sin^2(\frac{\xi_{r+1}-\xi}{2}) + \\ [\sin(\frac{\xi-\xi_{r-1}}{2}) \sin(\frac{\xi_{r+1}-\xi}{2}) + \sin(\frac{\xi_{r+2}-\xi}{2}) \sin(\frac{\xi-\xi_r}{2})] \sin(\frac{\xi_{r+2}-\xi}{2}), & \xi \in \Omega_{r+1}, \\ \sin^3(\frac{\xi_{r+2}-\xi}{2}), & \xi \in \Omega_{r+2}, \\ 0, & \text{otherwise}, \end{cases} \tag{10}$$

where $\theta = \sin(\frac{h}{2}) \sin(\frac{3h}{2}) \sin(h)$.
The following lemma provides $\mathcal{T}_r(\xi_m)$, $\mathcal{T}_r'(\xi_m)$ and $\mathcal{T}_k''(\xi_m)$.
Lemma [55]: The CTBS functions $\mathcal{T}_r(\xi_m)$ (10) and their derivatives at $\xi = \xi_m$ are given

as:

$$\mathcal{T}_r(\xi_m) = \begin{cases} \sigma_1, & \text{if } m = r+1 \text{ or } r-1, \\ \sigma_2, & \text{if } m = r, \\ 0, & \text{elsewhere,} \end{cases}$$

$$\mathcal{T}'_r(\xi_m) = \begin{cases} \sigma_3, & \text{if } m = r-1, \\ -\sigma_3, & \text{if } m = r+1, \\ 0, & \text{elsewhere,} \end{cases}$$

and

$$\mathcal{T}''_r(\xi_m) = \begin{cases} \sigma_4, & \text{if } m = r+1 \text{ or } r-1, \\ \sigma_5, & \text{if } m = r, \\ 0, & \text{elsewhere,} \end{cases} .$$

where $\sigma_1 = \frac{\sin^2(\frac{h}{2})}{\sin(\frac{3h}{2})\sin(h)}$, $\sigma_2 = \frac{2}{2\cos(h)+1}$, $\sigma_3 = \frac{3/4}{\sin(\frac{3h}{2})}$, $\sigma_4 = \frac{(3+9\cos(h))}{16\sin^2(\frac{h}{2})(2\cos(\frac{h}{2})+\cos(\frac{3h}{2}))}$ and $\sigma_5 = -3\cot^2(\frac{h}{2})4\cos(h)+2)$.
Thus using CTBS functions in Eq.(8), we get

$$\frac{\partial^k S_m}{\partial \xi^k}(\xi_r) = \sum_{i=1}^{N} a_{ri}^{(k)} S_m(\xi_i), \quad \text{for } m, r \in I_1, \quad \text{and } k = 1, 2,$$

which leads to the following matrix form:

$$P\vec{a}_r^{(k)} = Q_r^{(k)}, \tag{11}$$

where $\vec{a}_r^{(k)} = [a_{rm}^{(k)} : m \in I_1]$, $Q_r^{(k)} = [\frac{\partial^k S_l}{\partial \xi^k}(\xi_r) : l \in I_1]^T$, $P = [p_{rm} : r, m \in I_1]$ and

$$p_{rm} = \begin{cases} 2\sigma_1 + \sigma_2, & \text{if } r = m = 1 \text{ or } N, \\ \sigma_2, & \text{if } r = m \text{ and } 1 < r, m < N, \\ \sigma_1, & \text{if } (m = r-1 \text{ and } 2 < r \leq N) \text{ or } (r = m-1 \text{ and } 1 \leq m < N-1), \\ 0, & \text{elsewhere.} \end{cases}$$

The weighting coefficients $a_{rm}^{(k)}, r, m \in I_1$, are obtained by solving the system (11) through the well known efficient tridiagonal solver "Thomas algorithm". Eq. (11) gives to the following matrix form:

$$\mathbf{v}^{s+1} = \mathbf{C}\mathbf{v}^s + \mathbf{F}, \; s \geq 0, \tag{12}$$

where $\mathbf{C} = \mathbf{A}^{-1}\mathbf{B}$, $\mathbf{F} = \mathbf{A}^{-1}\mathbf{D}$

$$\mathbf{A} = \begin{bmatrix} a + ba_{11}^{(1)} - ca_{11}^{(2)} & ba_{12}^{(1)} - ca_{12}^{(2)} & ... & ba_{1N}^{(1)} - ca_{1N}^{(2)} \\ ba_{21}^{(1)} - ca_{22}^{(2)} & a + ba_{22}^{(1)} - ca_{22}^{(2)} & ... & ba_{2N}^{(1)} - ca_{2N}^{(2)} \\ . & . & ... & . \\ . & . & ... & . \\ . & . & ... & . \\ ba_{N1}^{(1)} - ca_{N1}^{(2)} & ba_{N2}^{(1)} - ca_{N2}^{(2)} & ... & a + ba_{NN}^{(1)} - ca_{NN}^{(2)} \end{bmatrix},$$

$$\mathbf{B} = \begin{bmatrix} d & 0 & ... & 0 \\ 0 & d & ... & 0 \\ . & . & ... & . \\ . & . & ... & . \\ . & . & ... & . \\ 0 & 0 & ... & d \end{bmatrix},$$

$a = \left(1 - \frac{\alpha\delta\mathsf{t}^{2-\beta}}{\mu_0 M(\alpha)(1-\beta)}\right)$, $b = \frac{\lambda\alpha\delta\mathsf{t}}{\mu_0 M(\alpha)}$, $c = \frac{\eta\alpha\delta\mathsf{t}}{\mu_0 M(\alpha)}$, $d = \left(\frac{\mu_0-\mu_1}{\mu_0} + \frac{\alpha\nu_1\delta\mathsf{t}^{2-\beta}}{\mu_0 M(\alpha)(1-\beta)}\right)$,
$\mathbf{v}^s = [v_0^s, v_1^s, ..., v_N^s]^T$ $\mathbf{D} = [d_1, d_2, ..., d_N]^T$,
$d_r = \sum_{j=1}^{s-1}\left(\frac{\mu_j-\mu_{j+1}}{\mu_0}\right) v(\xi_r, t^{s-j}) + \left(\frac{\mu_s}{\mu_0} v(\xi_r, t^0)\right) + \frac{\alpha\delta t^{2-\beta}}{\mu_0 M(\alpha)(1-\beta)}\left(\sum_{j=2}^{s}\nu_s v(\xi_r, t^{s-j+1}) + q(\xi_r, t^{s+1})\right)$.

3. Stability

Here, we assess the stability of the present method given in (12). Let $\mathcal{E}^s$ be the error between the approximate solution $\hat{v}^s$ and the exact solution v^s at sth time level i.e. $\mathcal{E}^s = v^s - \hat{v}^s$. Then error equation for the method (12) is given by

$$\mathcal{E}^{s+1} = \mathbf{C}\mathcal{E}^s,$$

where $\mathbf{C}$ is known as amplification matrix. If $\| \mathbf{C} \| \leq 1$ (see [63] and Lax-Richtmyer condition for stability) then method (12) will be stable. This condition is equivalent to $\sigma(\mathbf{C}) \leq 1$, where $\rho(\mathbf{C})$ represents spectral radius of the matrix $\mathbf{C}$ [63] and is defined as $\rho(\mathbf{C})$=$\max_{1\leq i\leq N} \mid \zeta_i \mid$ and ζ_i is an eigenvalue of $\mathbf{C}$. In the next section, we provide computational values of $\rho(\mathbf{C})$ for the parameters $\delta\mathsf{t}, N$, and α to demonstrate that the method (12) satisfies the stability condition.

4. Test Problems

This section is devoted to numerical simulation of the proposed method. Three examples are implemented using the spatial domain with $\gamma_1 = 0$ and $\gamma_2 = 1$ and $M(\alpha) = 1$ for validation of the present method (12). Error norms $\mathsf{L}_\infty, \mathsf{L}_2$, pointwise absolute error, spectral radius $\rho(\mathbf{C})$ and rate of convergence (RoC) [64] are computed to assess performance and reliability of the current technique. To compare our results with CBSCM [49], the

values of convection-diffusion coefficients λ, η, and β are used which are given in [49] and $\alpha \approx 1$. Initial/boundary conditions (2)-(3) are taken from the exact analytical solution. Corei3, 2.4GHz processor and 2GB RAM are used for simulation while computer run time (RT) is measured in seconds.

4.1 Example-1

In the first example, we take Eqs.(1)-(3) and the exact solution $u(\xi, \mathtt{t}) = (\mathtt{t}+1)^2 \sin(\pi\xi)$[49]. Then

$$f(\xi,\mathtt{t}) = \left(\frac{M(\alpha)(\exp(\frac{\alpha \mathtt{t}}{\alpha-1})(1-2\alpha)+\alpha(t+2)-1)}{\alpha^2} - \frac{t^{1-\beta}(2t(t+3)-\beta(2t+5)+\beta^2+6)}{(\beta-1)(\beta-2)(\beta-3)} \right)$$
$$\sin(\pi\xi) + \pi(\mathtt{t}+1)^2 \left(\kappa\cos(\pi\xi) - \nu\pi\sin(\pi\xi)\right).$$

Computations are carried out with different values of α, h, δt and results of the present method are provided in Tables 1-4 using $\lambda = 0.05$, $\eta = 0.4$, $\beta = 1/2$ [49]. In Table 1, pointwise absolute errors at various values of ξ are presented for $\alpha = 0.25, 0.5, 0.75, 0.95$, with $\delta t = 10^{-4}$, $h = 0.002$, and $t = 0.1$. Tables 2–3 report the L2, L∞ errors, spectral radius $\rho(\mathbf{C})$, runtime (RT), and rates of convergence of the proposed method at $t = 0.1$ for $\alpha = 0.25, 0.5$. Table 4 presents a comparison of the L2 and L∞ errors for $M = 10, 50, 100, 500$ and $\alpha = 1 - 10^{-4}$, with $\delta t = 10^{-4}, 10^{-5}$ and $h = 0.01$, alongside the results obtained using the CBSCM method [49]. Fig. 1 shows exact and approximate solutions using $\alpha = 0.25, 0.5, 0.75, 0.9$, $\delta t = 0.005$ and $h = 0.05$ over the space interval $[0, 1]$. Fig. 2 depicts behavior of the solution plotted in Fig. 1 over a small space interval. Fig. 3 shows surface plot of the computed solutions at different times t, $0 \le t \le 0.1$ with $\alpha = 0.5$, $\delta t = 0.005$ and $h = 0.05$.

Table 1: Absolute error versus α at $t = 0.1$ using $\delta t = 10^{-4}$ and $h = 0.002$

ξ	$\alpha = 0.25$	$\alpha = 0.5$	$\alpha = 0.75$	$\alpha = 0.95$
0.1	2.3090×10^{-6}	2.4380×10^{-6}	2.1814×10^{-6}	1.2954×10^{-6}
0.2	5.7425×10^{-6}	5.4219×10^{-6}	4.4510×10^{-6}	2.5014×10^{-6}
0.3	8.5385×10^{-5}	7.8344×10^{-6}	6.2730×10^{-6}	3.4645×10^{-6}
0.4	1.0446×10^{-5}	9.4527×10^{-6}	7.4733×10^{-6}	4.0897×10^{-6}
0.5	1.1301×10^{-5}	1.0131×10^{-5}	7.9380×10^{-6}	4.3150×10^{-6}
0.6	1.1040×10^{-5}	9.8133×10^{-6}	7.6252×10^{-6}	4.1179×10^{-6}
0.7	9.7122×10^{-6}	8.5442×10^{-6}	6.5689×10^{-6}	3.5173×10^{-6}
0.8	2.5714×10^{-6}	6.4595×10^{-6}	4.8763×10^{-6}	3.4744×10^{-6}
0.9	4.5521×10^{-6}	3.7768×10^{-6}	2.7173×10^{-6}	1.3717×10^{-6}

Table 2: L_2, L_∞ and RoC with $h = 0.002, t = 0.1$

α	δt	L_2	L_∞	$\mathsf{RoC}(\mathsf{L}_\infty)$	$\rho(\mathbf{C})$	RT
0.5	0.002	7.4147×10^{-6}	2.3453×10^{-4}	$---$	1.0	2.0723
0.5	0.001	3.7382×10^{-6}	1.1824×10^{-4}	0.9880	1.0	2.0408
0.5	0.0005	1.8575×10^{-6}	5.8753×10^{-5}	1.0090	1.0	2.5511
0.5	0.00025	9.0164×10^{-7}	2.8519×10^{-5}	1.0427	1.0	4.7765
0.25	0.002	8.2754×10^{-6}	2.6184×10^{-4}	$---$	1.0	1.8673
0.25	0.001	4.1728×10^{-6}	1.3203×10^{-4}	0.9878	1.0	2.0043
0.25	0.0005	2.0737×10^{-6}	6.5612×10^{-5}	1.0088	1.0	2.5864
0.25	0.00025	1.0068×10^{-6}	3.1855×10^{-5}	1.0424	1.0	4.8788

Table 3: L_2, L_∞ and RoC at $t = 0.1$using $\delta t = 0.000125$

α	h	L_2	L_∞	$\mathsf{RoC}(\mathsf{L}_\infty)$	$\rho(\mathbf{C})$	RT
0.5	0.05	2.2139×10^{-4}	1.3833×10^{-3}	$---$	1.0	0.4582
0.5	0.025	3.7852×10^{-5}	3.2332×10^{-4}	2.0971	1.0	0.8893
0.5	0.0125	5.7741×10^{-6}	5.7753×10^{-5}	2.4850	1.0	1.6376
0.5	0.00625	3.7145×10^{-7}	9.7241×10^{-6}	2.5703	1.0	3.4969

Table 4: L_∞ and L_2 for $\alpha = 1 - 10^{-4}, h = 0.01$

		CTBS-DQ		CBSCM[49]	
δt	M	L_∞	L_2	L_∞	L_2
10^{-4}	10	2.3777×10^{-7}	1.6813×10^{-8}	9.4351×10^{-6}	1.3253×10^{-7}
	50	1.1041×10^{-6}	7.8070×10^{-8}	1.1446×10^{-5}	3.3175×10^{-7}
	100	2.1475×10^{-6}	1.5185×10^{-7}	1.1943×10^{-5}	5.7312×10^{-7}
	500	9.6180×10^{-6}	6.8010×10^{-7}	3.5394×10^{-5}	2.4398×10^{-6}
10^{-5}	10	4.7593×10^{-8}	3.3653×10^{-9}	4.3771×10^{-6}	4.4106×10^{-8}
	50	1.4499×10^{-7}	1.0252×10^{-8}	8.2580×10^{-6}	9.5928×10^{-8}
	100	2.6654×10^{-7}	1.8847×10^{-8}	9.5573×10^{-6}	1.2493×10^{-7}
	500	1.2329×10^{-6}	8.7181×10^{-8}	1.1579×10^{-5}	2.2516×10^{-7}

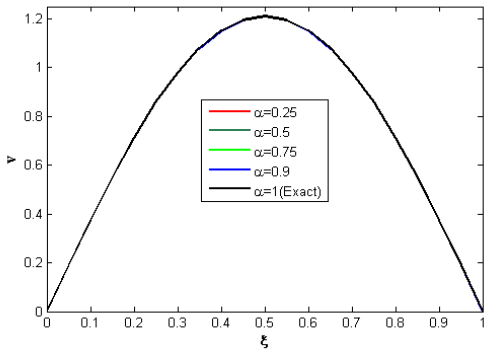

Figure 1: Exact and approximate solutions for $\delta t = 0.005, h = 0.05$

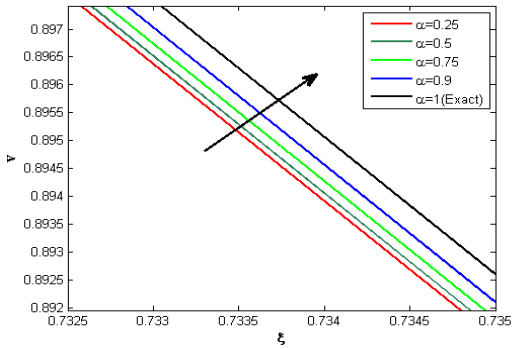

Figure 2: Exact and approximate solutions for $\delta t = 0.005, h = 0.05$

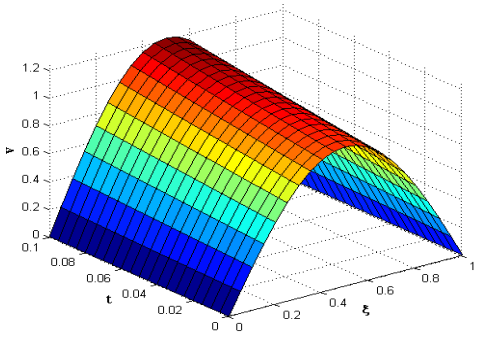

Figure 3: Approximate solutions for $\delta t = 0.005, h = 0.05, 0 \leq t \leq 0.1$

4.2 Example-2

Consider Eqs.(1)-(3) with exact solution $u(\xi, \mathrm{t}) = (\mathrm{t}+1)^2[1 - \cos 2\pi\xi + 2\pi^2\xi(1-\xi)]$[49]. Then

$$f(\xi,\mathsf{t}) = \left(\frac{2M(\alpha)(\exp(\frac{\alpha \mathsf{t}}{\alpha-1})(2\alpha-1)-\alpha(t+2)+1)}{\alpha^2} - \frac{t^{1-\beta}(2t(t+3)-\beta(2t+5)+\beta^2+6)}{(\beta-1)(\beta-2)(\beta-3)}\right)$$
$$\left(\cos(2\pi\xi)+2\pi^2\xi(\xi-1)-1\right)+(\mathsf{t}+1)^2\left(\kappa(2\pi\sin(2\pi\xi)+2\pi^2(1-2\xi))-\nu(4\pi^2\cos(2\pi\xi)-4\pi^2)\right).$$

Simulation is done using various values of α, δt, h and results of the present method are provided in Tables 5-8 using $\lambda = 0.005$, $\eta = 0.5$, $\beta = 1/3$ [49]. In Table 5, pointwise absolute errors at various values of ξ for $\alpha = 0.25, 0.5, 0.75, 0.95, \delta t = 10^{-4}, h = 0.002, t = 0.1$ are provided. In Tables 6-7, $\mathsf{L}_2, \mathsf{L}_\infty, \rho(\mathbf{C})$, RT, and rates of convergence of the suggested method at $t = 0.1$ for $\alpha = 0.5$ are given. Table 8 compares the error norms $\mathsf{L}_2, \mathsf{L}_\infty$ at different time levels M for $\alpha = 1 - 10^{-6}$, $\delta t = 10^{-4}, 10^{-5}$, $h = 0.01$ with the results of CBSCM [49]. Fig. 1 shows exact and approximate solutions using $\alpha = 0.75$, $\delta t = 0.005, h = 0.05$. Fig. 2 depicts error in solution obtained using $\alpha = 0.75$, $\delta t = 0.005, h = 0.05$. Fig. 3 displays surface plot of the numerical solutions at different times t, $0 \le t \le 0.1$ with $\alpha = 0.75$, $\delta t = 0.005$ and $h = 0.05$.

Table 5: Absolute error versus α at $t = 0.1$ using $\delta t = 10^{-4}$ and $h = 0.002$

ξ	$\alpha = 0.25$	$\alpha = 0.5$	$\alpha = 0.75$	$\alpha = 0.95$
0.1	1.1203×10^{-5}	1.0707×10^{-5}	9.5337×10^{-6}	7.0939×10^{-6}
0.2	1.6870×10^{-5}	1.5778×10^{-5}	1.3460×10^{-5}	8.8207×10^{-6}
0.3	1.8148×10^{-5}	1.6618×10^{-5}	1.3477×10^{-5}	7.2238×10^{-6}
0.4	1.7521×10^{-5}	1.5718×10^{-5}	1.2089×10^{-5}	4.8659×10^{-6}
0.5	1.7107×10^{-5}	1.5188×10^{-5}	1.1375×10^{-5}	3.8166×10^{-6}
0.6	1.7731×10^{-5}	1.5846×10^{-5}	1.2140×10^{-5}	4.8675×10^{-6}
0.7	1.8574×10^{-5}	1.6880×10^{-5}	1.3585×10^{-5}	7.2317×10^{-6}
0.8	1.7521×10^{-5}	1.6184×10^{-5}	1.3633×10^{-5}	8.8413×10^{-6}
0.9	1.2086×10^{-5}	1.1264×10^{-5}	9.7799×10^{-6}	7.1312×10^{-6}

Table 6: L_2, L_∞ and RoC at $t = 0.1$ with $h = 0.002$

α	δt	L_2	L_∞	RoC(L_∞)	$\rho(\mathbf{C})$	RT
0.5	0.002	2.1309×10^{-5}	6.1749×10^{-4}	$---$	1.0	2.1026
0.5	0.001	1.0491×10^{-5}	3.2831×10^{-4}	1.0323	1.0	2.2626
0.5	0.0005	5.0286×10^{-6}	1.5500×10^{-4}	1.0828	1.0	2.9344
0.5	0.00025	2.2819×10^{-6}	6.7775×10^{-5}	1.1936	1.0	5.2883

Table 7: L_2, L_∞ and RoC at $t = 0.1$ with $\delta t = 0.000125$

α	h	L_2	L_∞	RoC(L_∞)	$\rho(\mathbf{C})$	RT
0.5	0.05	1.6001×10^{-3}	1.2404×10^{-2}	$---$	1.0	0.5416
0.5	0.025	2.8046×10^{-4}	3.0793×10^{-3}	2.0101	1.0	1.0159
0.5	0.0125	4.7168×10^{-5}	7.3755×10^{-4}	2.0618	1.0	1.8947
0.5	0.00625	6.6359×10^{-6}	1.5141×10^{-4}	2.2839	1.0	3.9057

Table 8: L_∞ and L_2 for $\alpha = 1 - 10^{-6}, h = 0.01$

		CTBS-DQ		CBSCM[49]	
δt	M	L_∞	L_2	L_∞	L_2
10^{-4}	10	1.0000×10^{-4}	1.4380×10^{-6}	3.0131×10^{-5}	1.1709×10^{-6}
	50	1.0000×10^{-4}	1.7304×10^{-6}	3.3049×10^{-4}	2.0104×10^{-5}
	100	1.3501×10^{-4}	2.1011×10^{-6}	1.0609×10^{-3}	7.2658×10^{-5}
	500	2.3642×10^{-4}	3.9788×10^{-6}	2.1712×10^{-2}	1.5005×10^{-3}
10^{-5}	10	1.0000×10^{-5}	1.4295×10^{-7}	3.7552×10^{-7}	1.4690×10^{-8}
	50	1.0000×10^{-5}	1.7332×10^{-7}	5.0060×10^{-6}	2.5430×10^{-7}
	100	1.6378×10^{-5}	2.3661×10^{-7}	1.6837×10^{-5}	9.2099×10^{-7}
	500	2.6842×10^{-5}	1.7990×10^{-6}	$2,8412 \times 10^{-4}$	1.9062×10^{-5}

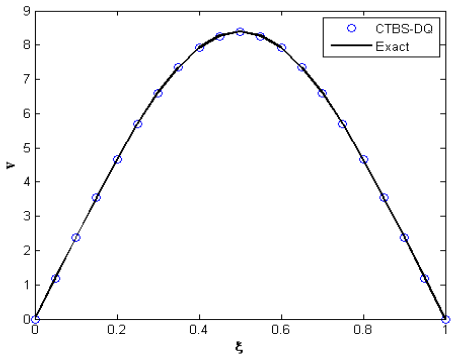

Figure 4: Exact and approximate solutions for $\alpha = 0.75, \delta t = 0.005, h = 0.05$

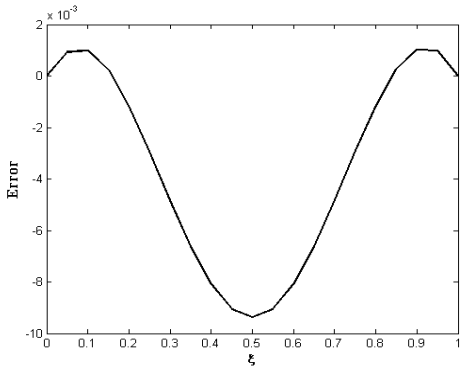

Figure 5: Exact and approximate solutions for $\alpha = 0.75, \delta t = 0.005, h = 0.05$

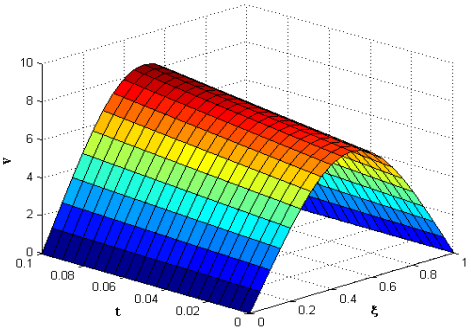

Figure 6: Approximate solutions for $\alpha = 0.75, \delta t = 0.005, h = 0.05, 0 \leq t \leq 0.1$

4.3 Example-3

In this example we take Eqs.(1)-(3) with exact solution $u(\xi, \mathsf{t}) = (\mathsf{t}+1)\cos(\pi\xi)$ [49]. Then
$f(\xi, \mathsf{t}) = \left(\frac{M(\alpha)}{\alpha}(\exp(\frac{\alpha \mathsf{t}}{\alpha-1}) - 1) - \frac{t^{1-\beta}(t-\beta+2)}{(\beta-1)(\beta-2)}\right)\cos(\pi\xi) - \pi(\mathsf{t}+1)(\kappa\sin(\pi\xi) - \nu\pi\cos(\pi\xi))$.
Computations are performed and the results are recorded in Table 8 for $\mathsf{L}_2, \mathsf{L}_\infty$ errors at $M = 10, 50, 100, 500$ using $\alpha = 1 - 10^{-6}$, $\delta t = 10^{-4}, 10^{-5}$, $h = 0.01$, $\lambda = 0.5$, $\eta = 0.005$, $\beta = 1/3$ along with the results of CBSCM [49]. In Fig. 7, plot of exact solution and approximate solutions at $t = 0.1$ for $\alpha = 0.25, 0.5, 0.75, 0.9$ using $\delta t = 0.005, h = 0.05$ are shown. In Fig. 8, surface plot of the approximate solutions at various times t, $0 \leq t \leq 0.1$ using $\alpha = 0.5$, $\delta t = 0.005$ and $h = 0.05$ is depicted.

Table 9: L_∞ and L_2 for $\alpha = 1 - 10^{-6}, h = 0.01$

		CTBS-DQ		CBSCM[49]	
δt	M	L_∞	L_2	L_∞	L_2
10^{-4}	10	1.0000×10^{-4}	1.4380×10^{-6}	3.0131×10^{-5}	1.1709×10^{-6}
	50	1.0000×10^{-4}	1.7304×10^{-6}	3.3049×10^{-4}	2.0104×10^{-5}
	100	1.3501×10^{-4}	2.1011×10^{-6}	1.0609×10^{-3}	7.2658×10^{-5}
	500	2.3642×10^{-4}	3.9788×10^{-6}	2.1712×10^{-2}	1.5005×10^{-3}
10^{-5}	10	1.0000×10^{-5}	1.4295×10^{-7}	3.7552×10^{-7}	1.4690×10^{-8}
	50	1.0000×10^{-5}	1.7332×10^{-7}	5.0060×10^{-6}	2.5430×10^{-7}
	100	1.6378×10^{-5}	2.3661×10^{-7}	1.6837×10^{-5}	9.2099×10^{-7}
	500	6.0528×10^{-5}	6.9515×10^{-7}	2.8412×10^{-4}	1.9062×10^{-5}

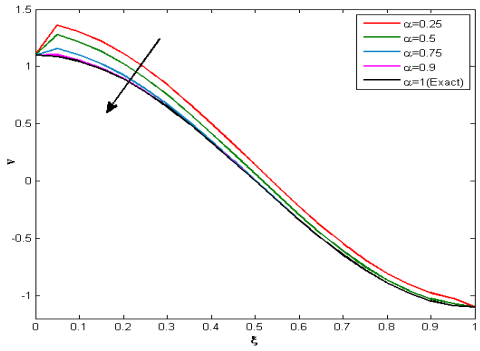

Figure 7: Exact and approximate solutions for $\delta t = 0.005, h = 0.05$

.

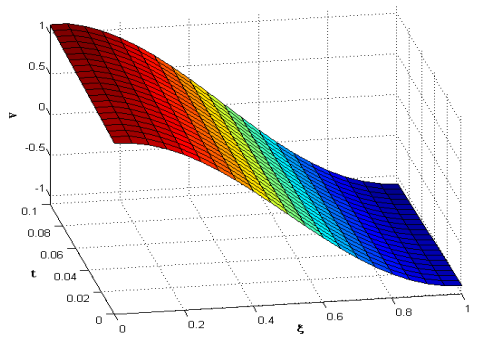

Figure 8: Exact and approximate solutions for $\delta t = 0.005, h = 0.05, 0 \leq t \leq 0.1$

5. Conclusion

The differential quadrature method based on cubic trigonometric B-spline functions is applied to solve convection-diffusion type fractional partial integro-differential equations, using the first-order method for the Caputo-Fabrizio derivative. The method is validated through three test problems. It demonstrates computational efficiency, and its accuracy and numerical convergence are analyzed for various time-step sizes, space-step sizes, and fractional orders. The stability of the method is discussed via spectral radius analysis. The proposed technique provided better accuracy compared to the cubic B-spline collocation method. Based on its excellent agreement with the exact solution, this approach is efficient, accurate, economical and stable to obtain approximate solutions of fractional PIDEs. The proposed method can be extended to multi-dimensional convection-diffusion models with variable coefficients. Additionally, incorporating other non-singular fractional operators could further enhance the model's flexibility and accuracy.

Declarations

Competing interests:
Authors declare no conflict of interest.
Availability of data and materials:
Data will be provided on request to the corresponding author.
Acknowledgements and Funding:
Aziz Khan and Thabet Abdeljawad would like to thank Prince Sultan University for paying the APC and supporting through TAS research lab.

References

[1] Hina Zahir, Javairia Gul, Mustafa Inc, Rubayyi T Alqahtani, et al. Impact of fractional magnetohydrodynamic and hall current on ree-eyring fluid flow by using radial basis function method. *Alexandria Engineering Journal*, 88:210–215, 2024.

[2] Shams Ul Arifeen, Sirajul Haq, and Ihteram Ali. Galerkin approximation of burgers-huxley equation with fractional order arising in reaction mechanism and diffusion transport. *Physica Scripta*, 99(12):125215, 2024.

[3] Hasib Khan, Altaf Hussain Rajpar, Jehad Alzabut, Muhammad Aslam, Sina Etemad, and Shahram Rezapour. On a fractal–fractional-based modeling for influenza and its analytical results. *Qualitative theory of dynamical systems*, 23(2):70, 2024.

[4] Saim Ahmed, Ahmad Taher Azar, Mahmoud Abdel-Aty, Hasib Khan, and Jehad Alzabut. A nonlinear system of hybrid fractional differential equations with application to fixed time sliding mode control for Leukemia therapy. *Ain Shams Engineering Journal*, 15(4):102566, 2024.

[5] Hajira Irshad, Mehnaz Shakeel, Imtiaz Ahmad, Hijaz Ahmad, Chutarat Tearnbucha, and Weerawat Sudsutad. Simulation of generalized time fractional gardner equation utilizing in plasma physics for non-linear propagation of ion-acoustic waves. *Thermal Science*, 27(Spec. issue 1):121–128, 2023.

[6] Shams Ul Arifeen, Sirajul Haq, Ihteram Ali, and Saud Fahad Aldosary. Galerkin approximation for multi-term time-fractional differential equations. *Ain Shams Engineering Journal*, 15(7):102806, 2024.

[7] Académie des Sciences (Paris). *Comptes rendus hebdomadaires des séances de l'Académie des sciences*, volume 78. Gauthier-Villars, 1874.

[8] Mehnaz Shakeel, Shahida Parveen, Siraj-ul Islam, and Iltaf Hussain. Numerical solution and characteristic study of time-fractional shocks collision. *Physica Scripta*, 96(4):045214, 2021.

[9] Shakeel Mehnaz, Muhammad Nawaz Khan, Imtiaz Ahmad, Sayed Abdel-Khalek, Ahmed Mohammed Alghamdi, and Mustafa Inc. The generalized time fractional gardner equation via numerical meshless collocation method. *Thermal Science*, 26(Spec. issue 1):469–474, 2022.

[10] Imtiaz Ahmad, Rashid Jan, Normy Norfiza Abdul Razak, Aziz Khan, and Thabet Abdeljawad. Exploring fractional-order models in computational finance via an efficient hybrid approach. *European Journal of Pure and Applied Mathematics*, 18(1):5793–5793, 2025.

[11] I. Podlubny. *Fractional Differential Equations*. Academic Press London, UK, 1999.

[12] Shams Ul Arifeen and Sirajul Haq. Petrov–galerkin approximation of time-fractional coupled korteweg–de vries equation for propagation of long wave in shallow water. *Mathematics and Computers in Simulation*, 207:226–242, 2023.

[13] Numerical solution of two dimensional time-fractional telegraph equation using chebyshev spectral collocation method. *Partial Differential Equations in Applied Mathematics*, 13:101129, 2025.

[14] Sirajul Haq, Shams Ul Arifeen, and Ayesha Noreen. An efficient computational technique for higher order kdv equation arising in shallow water waves. *Applied Numerical Mathematics*, 189:53–65, 2023.

[15] Shams Ul Arifeen, Sirajul Haq, and Farhan Golkarmanesh. Computational study of multiterm time-fractional differential equation using cubic b-spline finite element method. *Complexity*, 2022(1):3160725, 2022.

[16] Hasib Khan, Jehad Alzabut, JF Gómez-Aguilar, and Abdulwasea Alkhazan. Essential criteria for existence of solution of a modified-ABC fractional order smoking model. *Ain Shams Engineering Journal*, 15(5):102646, 2024.

[17] M. Caputo and M. Fabrizio. A new definition of fractional derivative without singular kernel. *Progress in Fractional Differentiation & Applications*, 1(2):1–13, 2015.

[18] J. Losada and J. J. Nieto. Properties of a new fractional derivative without singular kernel. *Progress in Fractional Differentiation and Applications*, 1(2):87–92, 2015.

[19] A. Atangana and B.S.T. Alkahtani. Extension of the resistance, inductance, capacitance electrical circuit to fractional derivative without singular kernel. *Advances in Mechanical Engineering*, 7(6):1–6, 2015.

[20] J. F. Gómez-Aguilar, H. Yépez-Martínez, C. Calderón-Ramón, I. Cruz-Orduña, R.F. Escobar-Jiménez, and V. H. Olivares-Peregrino. Modeling of a mass-spring-damper system by fractional derivatives with and without a singular kernel. *Entropy*, 17(9):6289–6303, 2015.

[21] A. Atangana and R.T. Alqahtani. Numerical approximation of the space-time Caputo-Fabrizio fractional derivative and application to groundwater pollution equation. *Advances in Difference Equations*, 2016:156, 2016.

[22] T. Abdeljawad and D. Baleanu. On fractional derivatives with exponential kernel and their discrete versions. *Reports on Mathematical Physics*, 80(1):11–27, 2017.

[23] M. Al-Refai. Reduction of order formula and fundamental set of solutions for linear fractional differential equations. *Applied Mathematics Letters*, 82:8–13, 2018.

[24] H. Yépez-Martínez and J.F. Gómez-Aguilar. A new modified definition of Caputo-Fabrizio fractional-order derivative and their applications to the multi step homotopy analysis method (MHAM). *Journal of Computational and Applied Mathematics*, 346:247–260, 2019.

[25] S. Qureshi, N.A. Rangaig, and D. Baleanu. New numerical aspects of Caputo-Fabrizio fractional derivative operator. *Mathematics*, 7:734, 2019.

[26] H. K. Jassim and M.A.S. Hussain. On approximate solutions for fractional system of differential equations with Caputo-Fabrizio fractional operator. *Journal of Mathematics and Computer Science*, 23:58–66, 2020.

[27] F. Jin, Zi-S. Qianand Yu-M. Chu, and M.U. Rahman. On nonlinear evolution model for drinking behavior under caputo-fabrizio derivative. *Journal of Applied Analysis and Computation*, 12:790–806, 2022.

[28] D.F. Jamil, S. Saleem, R. Roslan, F.S. Al-Mubaddel, M. Rahimi-Gorji, A. Issakhov, and S.U. Din. Analysis of non-Newtonian magnetic casson blood flow in an inclined stenosed artery using Caputo-Fabrizio fractional derivatives. *Computer Methods and Programs in Biomedicine*, 203:106044, 2021.

[29] W. Adel, Y.A. Amer, E.S.M. Youssef, and A.M.S. Mahdy. Mathematical analysis and simulations for a caputo-fabrizio fractional covid-19 model. *Partial Differential Equations in Applied Mathematics*, 8:100558, 2023.

[30] Imtiaz Ahmad, Rashid Jan, Normy Norfiza Abdul Razak, Aziz Khan, and Thabet Abdeljawad. Numerical investigation of the dynamical behavior of hepatitis b virus via caputo-fabrizio fractional derivative. *European Journal of Pure and Applied Mathematics*, 18(1):5509–5509, 2025.

[31] K. Dehingia, S. Boulaaras, and S. Gogoi. On the dynamics of a nutrient-plankton system with caputo and Caputo-Fabrizio fractional operators. *Journal of Computational Science*, 76:102232, 2024.

[32] R.P. Chauhan, S. Kumar, B.S.T. Alkahtani, and S.S. Alzaid. A study on fractional order financial model by using Caputo-Fabrizio derivative. *Results in Physics*, 57:107335, 2024.

[33] A. Kausar, Chuan-Y. Chang, M.A.Z. Raja, and M. Shoaib. A novel design of layered recurrent neural networks for fractional order Caputo-Fabrizio stiff electric circuit models. *Modern Physics Letters*, 39:2450393, 2025.

[34] H. Güng¨ör. A novel study on Caputo-Fabrizio fractional Cahn-Allen equation. *Alexandria Engineering Journal*, 119:1–7, 2025.

[35] Kanagaraj Muthuselvan, Baskar Sundaravadivoo, Shankar Rao Munjam, and Kottakkaran Sooppy Nisar. Novel exploration of topological degree method for nonin-

stantaneous impulsive fractional integro-differential equation through the application of filtering system. *Fixed Point Theory and Algorithms for Sciences and Engineering*, 2025(1):1, 2025.

[36] Siraj ul Islam, A. Ali, A. Zafar, and I. Hussain. A differential quadrature based approach for volterra partial integro-differential equation with a weakly singular kernel. *Computer Modeling in Engineering and Sciences*, 124:915–935, 2020.

[37] K. Khan, A. Ali, Fazal i Haq, I. Hussain, and N. Amir. A comparative numerical study of parabolic partial integro-differential equation arising from convection-diffusion. *Computer Modeling in Engineering and Sciences*, 126:673–692, 2021.

[38] A.K. Hussain, N. Rusli, F.S. Fadhel, and Z.R. Yahya. Solution of one-dimensional fractional order partial integro-differential equations using variational iteration method. *AIP Conference proceedings*, 1775(1):030096, 2016.

[39] Z. Avazzadeh, M.H. Heydari, and C. Cattani. Legendre wavelets for fractional partial integro-differential viscoelastic equations with weakly singular kernels. *The European Physical Journal Plus*, 134:368, 2019.

[40] O.A. Arqub. Numerical simulation of time-fractional partial differential equations arising in fluid flows via reproducing kernel method. *International Journal of Numerical Methods for Heat & Fluid Flow*, 30(11):4711–4733, 2019.

[41] H. Bazgir and B. Ghazanfari. Spectral solution of fractional fourth order partial integro-differential equations. *Computational Methods for Differential Equations*, 7(2):289–301, 2019.

[42] S. Arshad. B-spline solution of fractional integro partial differential equation with a weakly singular kernel. *Numerical Methods for Partial Differential Equations*, 33(5):1565–1581, 2017.

[43] J. R. Loha, P. Chang, and K.G. Tay. New method for solving fractional partial integro-differential equations by combination of laplace transform and resolvent kernel method. *Chinese Journal of Physics*, 67:666–680, 2020.

[44] J. Guo, D. Xu, and Qiu. A finite difference scheme for the nonlinear time-fractional partial integro-differential equation. *Mathematical Methods in Applied Sciences*, 43:1–21, 2020.

[45] T. Akram, Z. Ali, F. Rabiei, K. Shah, and P. Kumam. A numerical study of nonlinear fractional order partial integro-differential equation with a weakly singular kernel. *Fractal and Fractional*, 5:85, 2021.

[46] A.G. Atta and Y.H. Youssri. Advanced shifted first-kind chebyshev collocation approach for solving the nonlinear time-fractional partial integro-differential equation with a weakly singular kernel. *Computational and Applied Mathematics*, 41:381, 2022.

[47] Z. Luo, X. Zhang, S. Wang, and L. Yao. Numerical approximation of time fractional partial integro-differential equation based on compact finite difference scheme. *Chaos, Solitons and Fractals*, 161:112395, 2022.

[48] J. Mohapatra, A. Panda, and N.R. Reddy. A comparative study on some semi-analytical methods for the solutions of fractional partial integro-differential equations. *Fractional Differential Calculus*, 12:223–233, 2022.

[49] S. S. Siddiqi and S. Arshed. Numerical solution of convection-diffusion integro-

differential equations with a weakly singular kernel. *Joural of Basic and Applied Science Research*, 3(11):106–120, 2013.

[50] A. Ali, S. Ahmad, S.I.A. Shah, and F. Haq. A quartic B-spline colocation technique for the solution of partial integro-differential equations with a weakly singular kernel. *Science International*, 27(4):2953–2958, 2015.

[51] A. Ali, E. Rahman, Z. Jan, I. Hussain, and S. Ahmad. A meshless collocation method for the approximate solution of a partial integro-differential equation. *Sindh University Research Journal-SURJ (Science Series)*, 48(3):589–594, 2016.

[52] A. Fahim, M.A.F. Araghi, J. Rashidinia, and M. Jalalvand. Numerical solution of Volterra partial integro-differential equations based on Sinc-collocation method. *Advances in Difference Equations*, 2017(1):362, 2017.

[53] H.O. Al-Humedi and Z.A. Jameel. Combining cubic B-spline Galerkin method with quadratic weight function for solving partial integro-differential equations. *Journal of Al-Qadisiyah for Computer Science and Mathematics*, 12:9–20, 2020.

[54] K. Khan, A. Ali, I. Hussain, N. Amir, et al. A comparative numerical study of parabolic partial integro-differential equation arising from convection-diffusion. *Computer Modeling in Engineering & Sciences*, 126(2):673–692, 2021.

[55] M. Yaseen, M. Abbas, T. Nazir, and D. Baleanu. A finite difference scheme based on cubic trigonometric B-splines for a time fractional diffusion-wave equation. *Advances in Difference Equations*, 2017:274, 2017.

[56] M. Yaseen and M. Abbas. An eefficient computational technique based on cubic trigonometric B-splines for time fractional Burgers' equation. *International Journal of Computer Mathematics*, 97(3):725–738, 2020.

[57] M. Yaseen and M. Abbas. An efficient cubic trigonometric B-spline collocation scheme for the time-fractional telegraph equation. *Applied Mathematics-A Journal of Chinese Universities*, 35(3):359–378, 2020.

[58] M. Yaseen, M. Abbas, and M.B. Riaz. A collocation method based on cubic trigonometric B-splines for the numerical simulation of the time-fractional diffusion equation. *Advances in Difference Equations*, 2021, Article 210:1–19, 2021.

[59] A.R. Hadhoud, A.A.M. Rageh, and T. Radwan. Computational solution of the time-fractional Schrödinger equation by using trigonometric B-spline collocation method. *Fractal and Fractional*, 6:127, 2022.

[60] R. Noureen, M.N. Naeem, D. Baleanu, P.O. Mohammed, and M.Y. Almusawa. Application of trigonometric B-spline functions for solving caputo time fractional gas dynamics equation. *AIMS Mathematics*, 8:25343–25370, 2023.

[61] Said Zibar, Brahim Tellab, Abdelkader Amara, Homan Emadifar, Atul Kumar, and Sabir Widatalla. Existence, uniqueness and stability analysis of a nonlinear coupled system involving mixed ϕ-riemann-liouville and ψ-caputo fractional derivatives. *Boundary Value Problems*, 2025(1):8, 2025.

[62] G. Arora and V. Joshi. A computational approach using modified trigonometric cubic B-spline for numerical solution of Burgers' equation in one and two dimensions. *Alexandria Engineering Journal*, 57(2):1087–1098, 2018.

[63] Siraj ul Islam, S. Haq, and A. Ali. A meshfree method for the numerical solution of the

RLW equation. *Journal of Computational and Applied Mathematics*, 223:997–1012, 2009.

[64] A. Ali, F. Haq, I. Hussain, and U. Shah. A meshless method of lines for numerical solution of some coupled nonlinear evolution equations. *Interntional Journal of Nonlinear Sciences and Numerical Simulation*, 15(2):121–128, 2014.